Heterogeneous Catalytic Degradation of Diuron Using Algerian Sodium Montmorillonite

Salima Tlemsani, Zoubida Taleb, Laurence Pirault-Roy, Safia Taleb

Heterogeneous Catalytic Degradation of Diuron Using Algerian Sodium Montmorillonite

Salima Tlemsani, Zoubida Taleb, Laurence Pirault-Roy, and Safia Taleb*

S. Tlemsani, Z. Taleb, S. Taleb Laboratory of Materials & CatalysisFaculty of Exact Sciences
Djillali Liabès University
Site I, BP 89, Sidi Bel Abbès 22000, Algeria E-mail: safia.taleb@univ-sba.dz
L. Pirault-Roy
Institute of Chemistry of Poitiers: Materials and Natural ResourcesUMR CNRS
University of Poitiers
4 rue Michel Brunet, Poitiers, CEDEX 9 86073, France

Keywords: *catalytic oxidation, diuron, pesticide, sodium montmorillonite, wastewater*

Abstract: Diuron is categorized as a probable human carcinogen by the United States Environmental Protection Agency (EPA). This work is aimed to determine the optimal conditions for the catalytic degradation of Diuron in an aqueous solution with H_2O_2 using Algerian sodium Montmorillonite (Mont-Na) as the catalyst. The material is characterized before and after the experiment using X-ray diffraction, Fourier transform infrared (FTIR) spectroscopy, specific surface area (S_{BET}), elemental analysis, and thermal analysis (TGA/DTA). The surface charge is determined by measuring the point of zero charge. Tests with H_2O_2 without Mont-Na provide a 32% conversion rate after 8 h.

However, a mixture of 1 g Mont-Na and H_2O_2 increases the conversion rate to 91% after 180 min at 25 °C and pH 6.3. The Diuron disappearance is evidenced by high-performance liquid chromatography using a UV–vis detector (HPLC/UV–vis). Specifically, 3,4-dichloroaniline (DCA) is the only by-product. At the basic pH values 9 and 11, a conversion rate of 72.5% is achieved with a lower contact time of 150 min. A change in temperature toward higher values results in a decrease in the degradation rate. Overall, Algerian sodium Montmorillonite is used successfully for the heterogeneous catalytic degradation of Diuron from polluted water.

1. Introduction

The substantial use of chemical compounds is essential to achieve the social and economic goals of the global community. The current best practices demonstrate that they can be widely used with a high degree of safety. However, much remains to be done to ensure the environmentally friendly use of toxic chemicals in accordance with the principles of sustainable development and to improve the quality of human life.[1] Researchers and government entities need to explore solutions to mitigate a large amount of pollutants released into the environment, including pharmaceuticals and personal care products, in addition to endocrine disrupting compounds, alkylphenols, perfluorinated compounds, industrial organic chemicals, and pesticides.[2]

The need of modern industrial societies to increase their level of agricultural production has led to an increase in the use of pesticides. Herbicides applied in excess to fields cause serious problems. During their application, this can lead to a loss of biodiversity. In addition, intensive farming operations can potentially contaminate the groundwater with a variety of pesticides.[3] The level of global pesticide consumption is around 2 million tons per year (45% of which is used in Europe alone).[4] Recently, a study examined the presence of the water phase of the 31 target pesticides used for consumption.

The analysis within the ecological risk assessments revealed a high level of risk associated with the presence of pesticides in the aquatic environment, including the risk to organisms.[5] Diuron (3-(3,4-dichlorophenyl)-1,1-dimethylurea) is a substituted urea herbicide registered for both occupational and residential uses, and it is commonly used worldwide.[6] It is generally applied as a pre-emergent and nonselective herbicide in agricultural and nonagricultural sites.[7,8] Its half-life is about 370 days. Relatively high concentrations of this pollutant have been noted around the world.[9] The phenylurea herbicide Diuron is a priority substance in the European Water Framework Directive, specifically directive 2000/06/EC.[10,11]

According to the European Union regulations, the maximum authorized concentration of Diuron in drinking water is 0.1, and 4.5 μg L^{-1} according to the World Health Organization. Diuron is classified as a probable carcinogen in relation to human health by the United States Environmental Protection Agency.[12] As a result of its broad use, Diuron and its metabolites have been detected in the marine sediments, surface water, and groundwater derived from both agricultural and urbanized catchments. Microbial degradation is considered to be the primary mechanism of Diuron dissipation from soil and water.[13,14] It is, therefore, necessary to apply appropriate techniques to reduce and minimize the leaching of herbicides from the application sites. Various methods have been proposed and among them are advanced oxidation processes (AOPs), membrane technology, adsorption, and ozonation.[15] Advanced oxidation processes are radical-mediated oxidation processes that have the capability to enable the complete mineralization of organic compounds. They are often called “zero sludge” processes. The types of AOP depend on the type of chemicals used, in addition to the specific technique and catalyst used in the process of the ultimate goal of oxidizing, thereby, mineralizing the target pollutant or compound.[16]

Advanced oxidation processes are widely reported for the degradation of several pesticides. To our knowledge, Diuron has been reviewed and compared for degradation using ozone + H_2O_2,[17] photocatalysis,[18] and chemical oxidation.[19] Catalytic transformations as efficient and environmentally friendly protocols have been broadened as a promising avenue in academic research laboratories and the chemical industry.

The use of heterogeneous nanocatalysts is a promising method, and it presents a promising option for the synthesis of organic compounds to obtain exceptional performance in terms of high activity, simple recovery, and recycling.[1,20] Clays possess certain properties which make them an ultimate choice as adsorbents or a catalysis support. This is due to their low cost, and high mechanical and

chemical stability.[18] Montmorillonite (MMT) clays have a 2:1 aluminosilicate layered structure with high surface areas. It is a kind of nanoclay due to the characteristics of the minerals.[20,21] Generally, whatever the application is, the degradation or adsorption efficiency strongly depends on the catalyst origin and properties, as well as on the operational conditions.[18] To date, Algerian Montmorillonite has been explored in relation to the adsorption of organic pollutants, such as methylene blue,[22] fluoride,[23] and chlorobenzene.[24] However, the oxidative removal of Diuron has not yet been studied. The oxidation processes in the liquid phase in the presence of H_2O_2 are known to be highly effective and it is important to emphasize that the use of this oxidant alone is not effective for most organic products.[25] The main objective of this study was the determination of the catalytic properties of Algerian sodium Montmorillonite (Mont-Na) by using it in the degradation of Diuron from water samples in the presence of H_2O_2. The catalyst was characterized using different techniques, and the metabolites produced during the process were also reported using high-performance liquid chromatography coupled to an ultraviolet–visible detector (HPLC/UV–vis).

2. Experimental Section

2.1. Materials

The clay chosen in this study was sodium Montmorillonite (Mont-Na) obtained from an Algerian company (National Company of Non-Ferrous Mining Products, ENOF). It was prepared from raw bentonite mixed with 3% of Na_2CO_3. Diuron (98% pure; $C_9H_{10}Cl_2N_2O$) was purchased from Sigma-Aldrich (Poitiers, France) and used as a pollutant. The aqueous solution of the Diuron at different concentrations was covered with aluminum foil and was prepared in darkness by dissolving the required proportion of Diuron (20 mg L^{-1}) in distilled water under heating without reaching the boiling temperature of Diuron (180 °C). The study of its UV spectrum allowed for the determination of the maximum adsorption wavelength, λ_{max}, of the order of 248 nm.

2.2. Characterization of the Catalyst (Mont-Na)

The interlayer distance d_{hkl} of the material was detected by X- ray diffraction (XRD) (EMPYREAN PANalytical diffractometer, France) operated at the $K\alpha$ copper wavelength (λ = 1.5406) and coupled with an Xcelerator linear detector.

To identify the bands that characterize the normal modes of vibration, and the remarkable functional groups present in Mont- Na, Fourier transform infrared spectroscopy was performed (Perkin Elmer FTIR Spectrometer Frontier, Algeria).

The specific surface (S_{BET}) of Mont-Na was estimated using the Brunauer, Emmett, and Teller (BET) method. The textural measurements were realized using a volumetric adsorption device (Micromeritics Smart VacPrep type, France). The S_{BET} surface area was calculated by the nitrogen gas adsorption/desorption isotherms at 77 K under standard pressure conditions.

The mass content (%) of carbon, nitrogen, and hydrogen in the clay samples was determined using C.H.N.S elemental analysis (Flash 2000, Thermo, France) after combustion.

The thermal analysis (TGA/DTA) was carried out under argon in a temperature range of 20–500 °C with a heating rate of 20 °C min^{-1}. This was done using a thermal analysis device (SDT Q66 V8.3, France).

The adsorption properties of an adsorbent depend largely on its surface charge. This indicates the acidic or basic character of its surface. To analyze the surface charge of Mont-Na, the point of zero charge (pH_{pzc}) was measured by following the method by Babic.[26] Six flasks, each filled with 50 mL of 0.1 N KCl and an adjusted pH of 2–12 using HNO_3 (0.1 N) and a NaOH solution (0.1 N). Following this, 0.05 g of Mont-Na was added to each of the flasks. The solutions were stirred overnight. The next day, the final pH of the solutions was recorded and was plotted as a function of the initial pH. The pH at which the change is negligible was considered to be the pH_{pzc}.

2.3. Methodology of Oxidation Experiments

2.3.1. Experimental System

Batch oxidation experiments were performed in the Laboratory of Materials and Catalysis (LMC) in Algeria to study the effect of different physicochemical parameters on Diuron–Mont-Na interactions. The amount of Mont-Na catalyst was modified from 0.5 to 2 g, contact time from 30 to 270 min, 2 < pH < 11 and temperature between 25 and 45 °C. The initial concentration of Diuron used was 20 mg L^{-1} prepared in 50 mL distilled water, Diuron/H_2O_2 (1:1 molar ratio) The samples were centrifuged (Centrifugal Apagee Swing 3000 centrifuge) and then filtered by syringe filters (0.45 µm) to obtain cleaner samples for the purpose of eliminating the interference caused by Mont-Na. The filtrates were finally analyzed using UV–vis spectrophotometry (PERKIN ELMER-Lambda 45 type).

The conversion of Diuron was calculated according to the following equation

$$\% \text{ Conversion} = [(C_0 - C_e) / C_0] \times 100 \quad (1)$$

where C_0 and C_e (mg L^{-1}) are the initial and equilibrium Diuron concentrations, respectively.

2.3.2. High-Performance Liquid Chromatography Coupled to an Ultraviolet Visible Detector (HPLC/UV–Vis)

The Diuron oxidation tests were carried out using HPLC/UV–vis (Shimadzu Prominence UFLCXR, France) on an Aminex HPX- 87H column. Isocratic elution was done using CH_3OH/H_2O 40– 60% v/v as a mobile phase. The injection volume and flow rate of the eluent were 20 µL and 1 mL min^{-1}, respectively. The temperature was maintained at 20 °C. Detection was performed across a continuum of wavelengths in the range of 205, 209, 210, and 248 nm. The device was fitted to a data logging station using the LabSolution software. At the end of each oxidation test, the main by-products of the reaction were identified.

3. Results and Discussion

3.1. Characterization of Mont-Na before and after DiuronDegradation Experiments

3.1.1. Point of Zero Charge pH_{pzc}

As shown in **Figure 1**, the results indicate that the pH_{pzc} value for Mont-Na was 7.8. When the pH is lower than the value of pH_{pzc}, the surfaces are positively charged and can release cations. When the pH is higher than the value of pH_{pzc}, the surfaces are negatively charged and can fix cations.[26] The pH_{pzc} value of Mont-Na in the previous work was 5.11.[26]

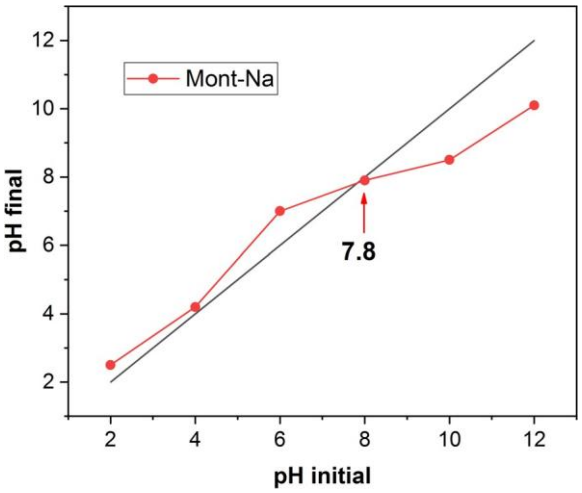

Figure 1. Determination of pH_{pzc} of Mont-Na

3.1.2. XRD

X-ray diffraction was carried out for Mont-Na before and after the catalytic oxidation of Diuron (Mont-AO). The spectrum presented in **Figure 2**A of Mont-Na indicates the presence of certain lines linked to crystalline impurities such as those found in quartz, granite (mica and feldspar), calcite, etc., in addition to the lines relating to Montmorillonite. Through the X-ray diffractogram, the predominant peaks are those of α-quartz type silica SiO_2 (2θ =27°), and Montmorillonite (5°). In addition, characteristic illite peaks (9° and 29.36°) were observed.[26]

The diffractogram of Mont-Na shows a basal spacing of 12.29 Å. Previously, the examination of the diffractogram of the local clay (Mont-N) also indicated a grating distance of 12.6 Å.[25] In the diffractogram of Mont-AO in the presence of the oxidant H_2O_2, a decrease in the basal distance of Mont-Na was observed, from 12.6 to 11.5 Å. This is probably due to the retention of Diuron on the Mont-Na surface because of the large size of the pollutant molecule compared to its interfoliar space or due to the exchangeable cations of Montmorillonite.

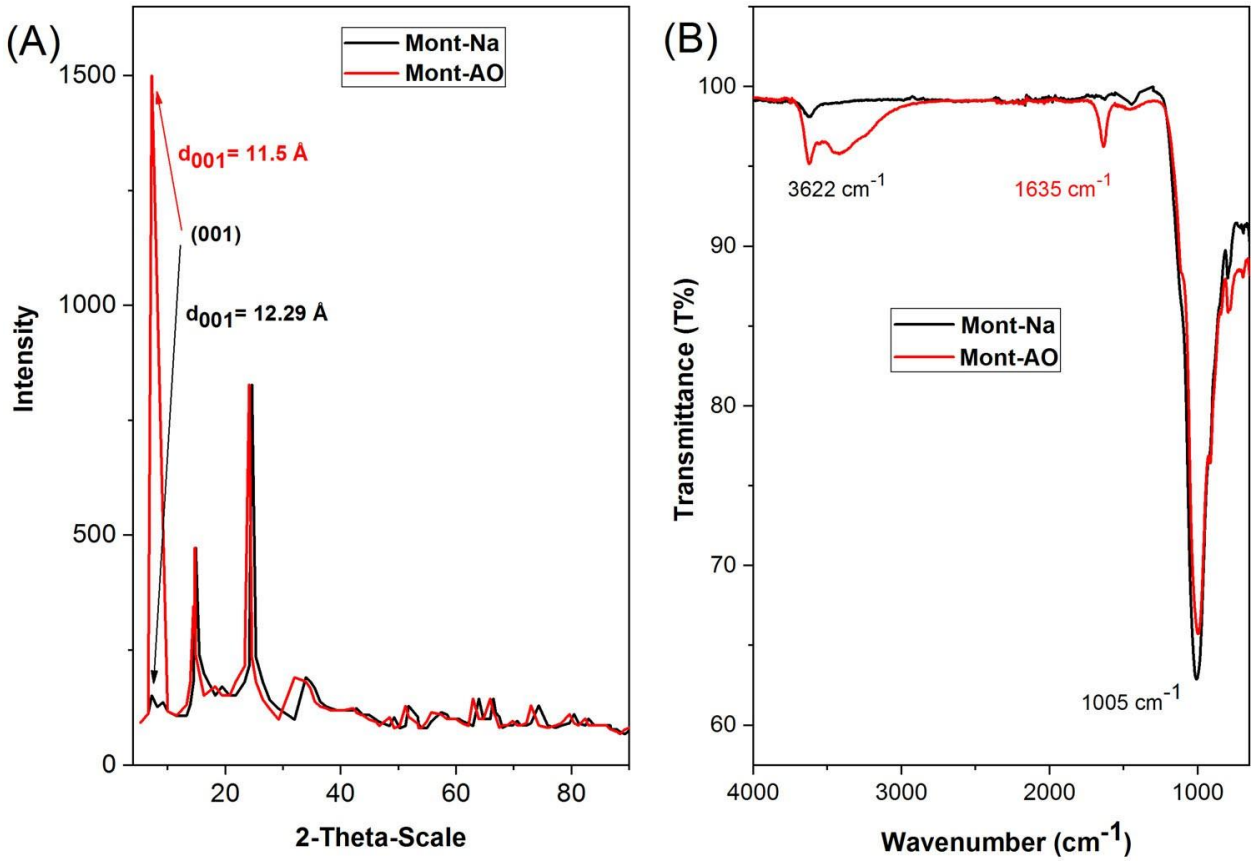

Figure 2. A) X-ray diffractograms of Mont-Na and Mont-AO, B) FTIR spectra of Mont-Na and Mont-AO.

3.1.3. FTIR Study

The spectrum of Mont-Na in Figure 2B represents the two absorption bands characterizing the OH bonds with a peak at 3622 cm^{-1}, related to the characteristics of Montmorillonite.[27] The recorded spectrum represents an absorption band centered at 1005 cm^{-1}. This band characterizes the stretching vibrations of the Si–O bond and the low intensity band at 1450 cm^{-1} is characteristic for carbonate ions (CO_3^{2-}). The IR spectrum of the Mont-AO sample shows a slight decrease in the intensity of the band corresponding to CO_3^{2-}. In parallel, the characteristic bands for the valence and deformation vibrations of the various groups of Diuron are assigned between 3300 and 3200 cm^{-1} attributed to the valence vibrations (stretching) of the NH bond. The C═O bond is around 1650 cm^{-1}, therefore the pollutant is well retained by Mont-Na.

3.1.4. Specific Surface Area (S_{BET})

It should be noted that the BET equation is generally applicable only over a certain range of relative pressures (between 0.05 and 0.35) where the theoretical and practical curves agree. As is presented in **Table 1**, the specific surface of Mont-Na increased after the oxidation of Diuron from 43 to 65 $m^2 g^{-1}$. This supports the probability of Diuron adsorption occurring on the surface of Mont-Na. The

micropore volume also increased. This can be explained by the elimination of impurities like carbonates as also shown in the IR spectrum of Mont-AO.

Table 1. Specific surface area (S_{BET}) values of Mont-Na and Mont-AO.

Sample	Mont-Na	Mont-AO
S_{BET} [$m^2\ g^{-1}$]	43	65
Volume of micropores [$cm^3\ g^{-1}$]	0.007	0.016
Pore diameter [Å]	69	51

3.1.5. C.H.N.S Elemental Analysis

According to **Table 2**, the results indicate that the dominant elements were carbon and hydrogen. The mass percentage of carbon decreased after the catalytic degradation of Diuron onto Mont-Na, indicating the probability of breaking one of the functional groups linked to carbonate ions CO_3^{2-}. This is in agreement with the IR spectrum of Mont-AO and the textural measurements.

Table 2. Elemental analysis in mass fractions.

Clay support	Nitrogen [N]	Carbon [C]	Hydrogen [H]
Mont-Na	0.00	0.51	0.76
Mont-AO	0.00	0.32	1.38

3.1.6. Thermal Analysis

The thermogravimetric analysis (TGA) of endothermic reactions consists of different stages corresponding to the loss of different water behaviors. In Zone 1 (<100 °C), the first step corresponds to the elimination of hygroscopic water (departure of water molecules free from hydration) at a low temperature. Zone 2 (at 450 °C) is where the second level corresponds to the loss in weight associated with the departure of water adsorbed in the interfoliar space. Zone 3 (at *T* around 600 °C) is the last step that corresponds to the elimination of water from which clay is formed, in addition to the dehydroxylation of the sheets' OH^- and the structure of the clays (crystalline water) adsorbed in the interfoliar space.[28] In Figure 3A, for Mont-Na, two levels were noticed. An endothermic peak at 90 °C was found to be associated with a weight loss of about 1.8%. The latter is related to the elimination of the physisorbed water on the surfaces of the particles. A second endothermic peak around 450 °C was accompanied by a weight loss of about 2.3%. This peak corresponds to the water adsorbed in the interfoliar space. The curves of the TGA/DTA analysis of Mont-Na after Diuron oxidation in Figure 3B shows that the thermogravimetric evolution also included the two endothermic stages discussed previously, in addition to the third between 120 and 160 °C relative to the melting point of Diuron (158.5 °C). The weight loss corresponding to this step for Mont-AO was 3.41%. The loss of mass produced by the increase in temperature is attributed to the desorption of the

surface and/or structural water formed due to the presence of Diuron.

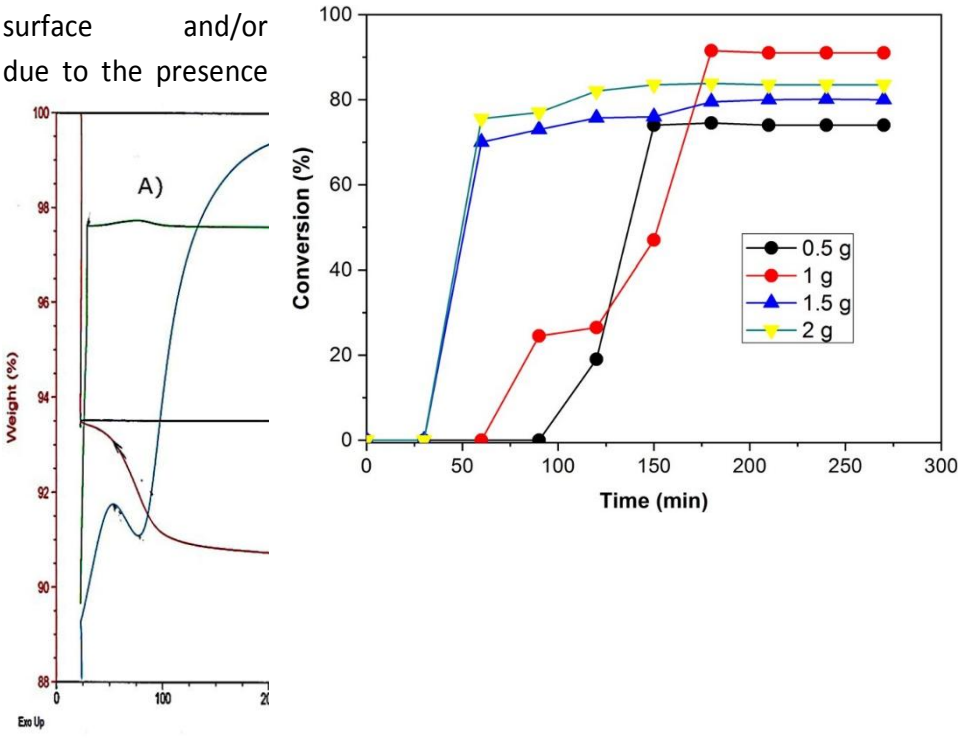

Figure 3. Thermogravimetric analysis of: A) Mont-Na, B) Mont-AO.

3.2. Catalytic Oxidation Studies in the Presence of H_2O_2

3.2.1. Effect of the Catalyst Amount and Contact Time

First, Diuron degradation kinetics have been studied in relation to different amounts of Mont-Na (0.5, 1, 1.5, and 2 g) over 270 min in order to optimize the appropriate amount and reaction time in further experiments. The initial concentration of Diuron used was 20 mg L^{-1} at room temperature and a medium pH value. Before the catalytic degradation process, Mont-Na was tested as an adsorbent. Despite the addition of 1 g of Mont-Na to the Diuron solution during a contact time of 61 h, no adsorption and therefore no results were obtained. Moreover, the experiments with H_2O_2 were realized due to Mont-Na. The oxidation test resulted in a conversion of 30% after 8 h. However, the use of Mont-Na as a catalyst of the H_2O_2 oxidation of Diuron resulted in an increasing rate of Diuron degradation such has been noticed in (Figure 4). The conversion rate increased due to increasing the catalyst amount from 0.5 to 1 g. In this last case, 91% of the conversion rate was obtained after 180 min of stirring. Beyond this time, the conversion remained constant. The conversion rate decreased slightly at 83.5% when the amount of Mont-Na was higher than 1 g. In this case, conversion was reached at 120 min.

Figure 4. Effect of the catalyst amount and contact time on the catalytic oxidation of Diuron (20 mg L^{-1}). T = 25 °C, pH 6.3, Diuron/H_2O_2 (1:1 molar ratio), $V_{solution}$ = 50 mL.

The previous study on Diuron oxidation by the coupled ozone-hydrogen peroxide was done under the chosen experimental conditions: C_0 = 5 mg L^{-1}, reaction time = 30 min, ozone applied = 6 mg L^{-1}, pH 7. The study indicated that Diuron was degraded by ozone along at a conversion of 80%, whereas it reached 90% in the presence of hydrogen peroxide.[17]

3.2.2. Effect of Temperature

The oxidation kinetics in the presence of 1 g of Mont-Na at 25, 35, and 45 °C at a fixed reaction time of 180 min is shown in Figure 5. The conversions increase quickly at 60 min when the temperature was higher than 35 °C. The maximum point of the conversions was 62.5% at 35 °C after 150 min and at 55.5% after 60 min at a temperature of 45 °C. This indicates that the increase in temperature diminishes the degradation of the pollutant by sodium Montmorillonite. Furthermore, it has been demonstrated in the previous research that the optimal biodegradation of Diuron by *Pseudomonas aeruginosa* FN was obtained at T = 25 °C using an initial Diuron concentration of (0.5 mg L^{-1}) and an initial optical density of 0.2.[4]

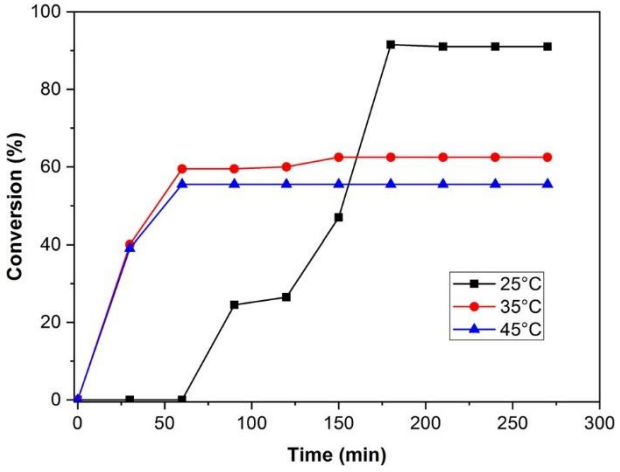

Figure 5. Effect of temperature on the catalytic oxidation of Diuron (20 mg L^{-1}). pH 6.3, Diuron/H_2O_2 (1:1 molar ratio), catalyst weight = 1 g, $V_{solution}$ = 50 mL, contact time = 180 min.

3.2.3. Effect of pH

The pH had a significant effect on the oxidation rate of the organic compounds. For this, the kinetics of the catalytic degradation of Diuron using Mont-Na have been studied by varying the pH of the system from 2 to 11. These were adjusted by adding the NaOH (0.1 M) and HCl (0.1 M) solutions. The presented results in Figure 6 show that degradation is favorable in a basic medium. In the presence of Mont-Na, the pH of the medium (pH 6.3) was more optimal for a good conversion (91%). At the basic pH values 9 and 11, a conversion rate of 72.5% was achieved with a lower contact time of 150 min. However, the Diuron oxidation gradually decreased at the acidic pH values 2 and 4, and a conversion rate of 35% was obtained after 180 min.

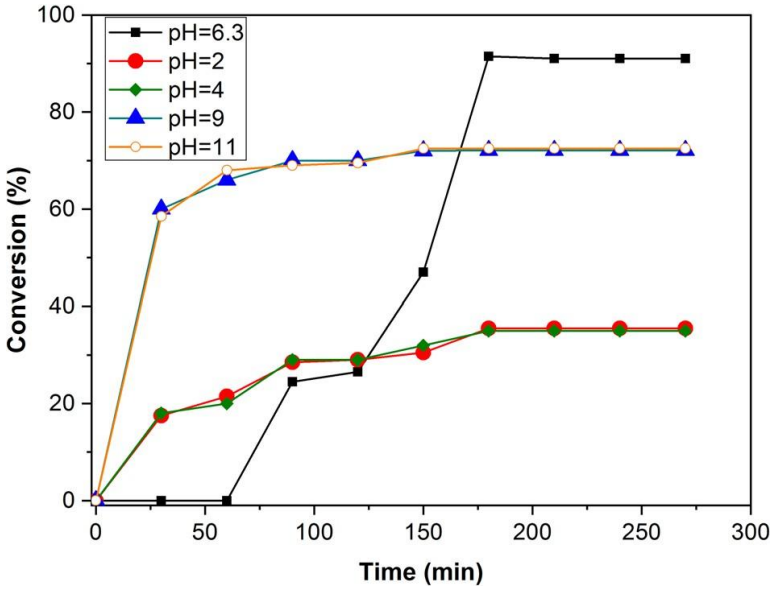

Figure 6. Effect of pH on the catalytic oxidation of Diuron (20 mg L^{-1}). T = 25 °C, Diuron/H_2O_2 (1:1 molar ratio), catalyst weight = 1 g, $V_{solution}$ = 50 mL, contact time = 180 min.

The results can be explained by the pH_{pzc} value of Mont-Na (Figure 1) and by understanding the behavior of Diuron in both acidic and basic environments. The pH_{pzc} value of Mont-Na was 7.8. It is

specified previously that at pH < pH_{pzc}, the surface of the material remains positively charged.[29] This means that it has more affinity with the molecular form of Diuron. This explains the strong degradation at pH 6.3. At pH > 9, the best rate of conversion is probably due to the precipitation of Diuron under extreme alkaline conditions and not the increased inter action with the Mont-Na surface. Moreover, Diuron molecules ($C_9H_{10}Cl_2N_2O$) have strongly negative polar regions corresponding to pairs of the oxygen atom. This is as well as very positive polar hydrogen atoms around the N–H group. Therefore, the oxygen and N–H groups can be considered highly polar and potential hydrogen bond acceptors and donors.[30] In the previous research, the efficiency of the photocatalytic Diuron degradation depended on the initial pH of the solution to be irradiated.

The best photocatalytic activity was obtained without modifying the initial pH (6.8) of the Diuron solution (20 mg L^{-1}). This was the case with the catalytic degradation onto Mont-Na. In general, the best degradation efficiencies of Diuron have been obtained at the initial pH values between 5 and 8.[31]

3.2.4. Analysis of the Samples after the Catalytic Oxidation ofDiuron by (HPLC/UV–Vis)

Oxidation processes do not always make it possible to achieve the complete mineralization of phytosanitary substances. This generally results in the formation of by-products whose molecular structure is close to that of the initial compound.[17] This work aimed to examine the evolution of Diuron during its oxidation through Mont-Na. The results of the previous work related to the oxidation of the other phenylureas enabled us to formulate hypotheses on the reaction mechanisms and the compounds likely to form from Diuron, whose wavelength is λ = 248 nm.[17] It seems that three degradation paths are possible: an attack on the methyl groups or dimethylation with the formation of *N*"(3,4-dichlorophenyl)-*N*-(methyl)-urea (DCPMU) and of *N*"-(3,4-dichlorophenyl)-urea (DCPU), λ = 210 nm, an attack on the chlorine atoms or dehalogenation to lead to *N*'(3-chloro- 4-hydroxyphenyl)-*N*-(methyl)-urea and to the chloride ion, λ =209 nm, or an attack on the amide group with a formation in the final stage of dichloroaniline and nitrate at λ = 205 nm.[32]

The formation of the main by-products of Diuron using the visible UV spectrophotometer could not have been detected because of the presence of the second band corresponding to phenol. Its maximum wavelength is around 110 nm, which is close to that of the by-products. At the end of each test, the main reaction products were identified using HPLC/UV–vis.

The criteria used for the identification of the by-products include the retention time (±0.05 min), and the detection on a continuum of wavelengths in the range of 205, 209, 210, and 248 nm corresponding to DCA, DCPMU, DCPU, and Diuron, respectively. Under the experimental conditions used, a residual of Diuron and the presence of DCA as the only by-products were observed. Notably in **Figure 7**, which shows the chromatogram relating to the Diuron oxidation detailed previously by Mont-Na with a 91% conversion rate, after 180 min of stirring at 25 °C and at the pH of the medium, the disappearance of Diuron and its transformation into 3,4-dichloroaniline (DCA) was demonstrated. An appropriate mechanism is proposed in **Figure 8**. Previously, by monitoring the metabolites, it was determined that the chemical oxidation process irreversibly resulted in 3,4-dichloroaniline as the only by-product.[19] In addition, it has been proven that few bacterial isolates degrading Diuron have

been described to date. Most of them partially degraded Diuron, giving rise to the metabolite 3,4-DCA.[13]

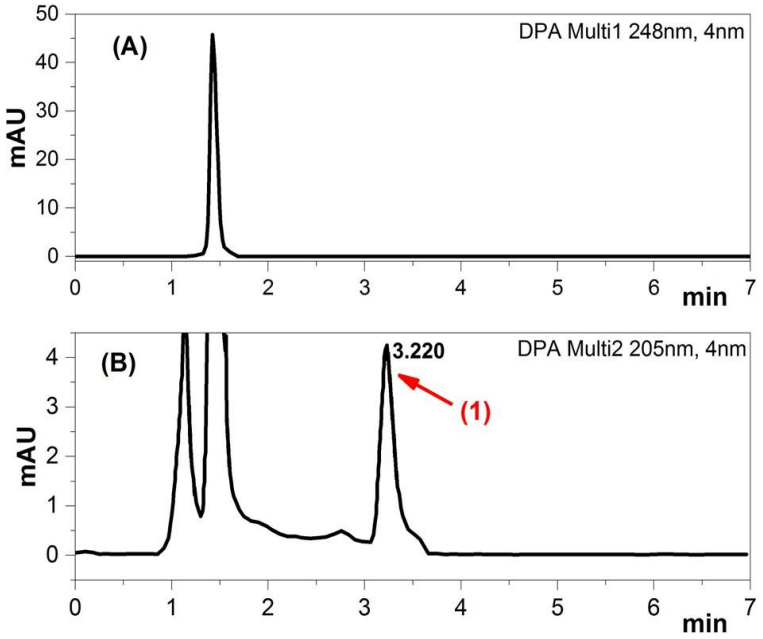

Figure 7. Chromatogram of Diuron degradation by Mon-Na, detected at a) λ = 248 nm b) λ = 205 nm, PICS: DCA (1). Mobile phase: water:CH_3OH/H_2O 40–60% v/v; flow rate: 1 mL min^{-1}; injection volume: 20 µL.

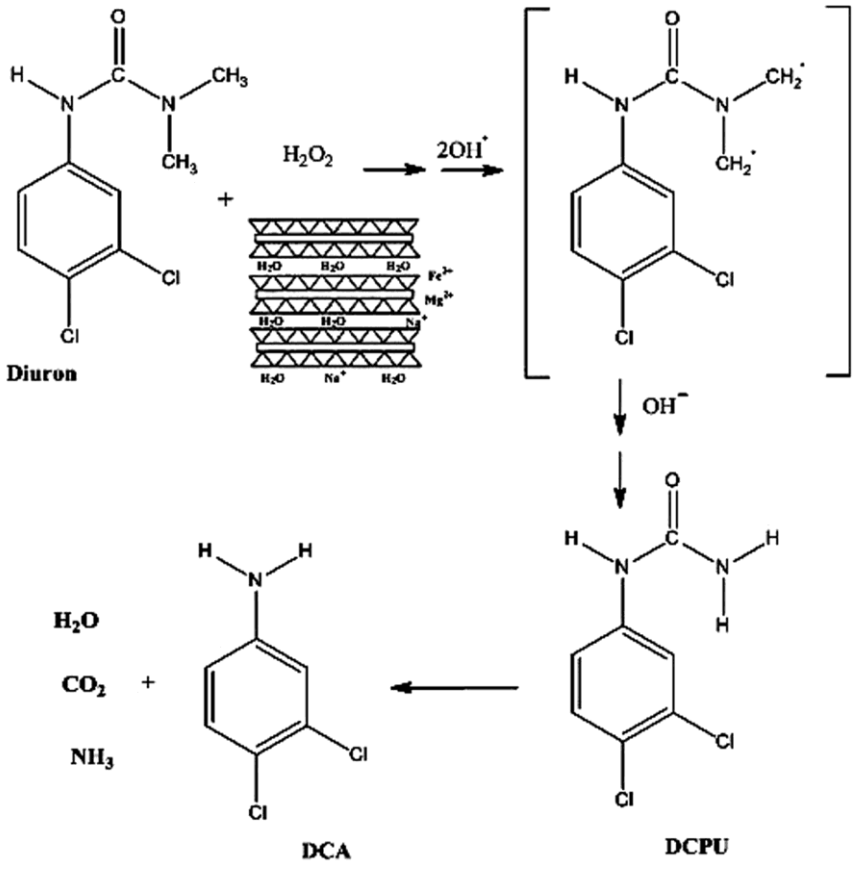

Figure 8. Mechanism of heterogeneous catalytic degradation of Diuron onto Mont-Na.

4. Conclusion

The focus of the present study was to assess the feasibility of Algerian sodium Montmorillonite in the catalytic oxidation of Diuron in the presence of oxygen peroxide. Using H_2O_2 to oxidize Diuron without the Mont-Na catalyst resulted in a conversion of 30% after 8 h in the experiment. Specifically, 91% Diuron degradation was obtained using 1 g of Mont-Na after 180 min of stirring in the presence of H_2O_2 at 25 °C and pH 6.3. The beneficial effect of basic pH was highlighted. In this case, the Diuron conversion was 72.5%. The increase in temperature decreased the degradation conversion. To identify the by-products formed during the reaction, the samples were analyzed using HPLC/UV–vis. The results prove that Diuron completely disappeared and transformed into 3,4-dichloroaniline (DCA). Possible modifications of the structural, textural, and chemical properties of Mont- Na were detected after the catalytic degradation of Diuron using several techniques (X-ray diffraction, Fourier transform infrared spectroscopy, thermogravimetric analysis, elemental analysis, and specific surface area). This affirms the retention of the pollutant by this material. Thus, although Mont-Na is a sustainable and efficient catalyst particularly for Diuron removal, evidently more Mont-Na is needed in a tertiary treatment plant to ensure the complete removal of the pollutants as its efficiency decreases with its reuse in successive degradation cycles. This study suggests that it is possible to further improve Algerian Montmorillonite's performance in the future through different pillaring techniques.

Acknowledgements

The Algerian Directorate General of Scientific Research and Technological Development (DGRSDT), and the Algerian Ministry of Higher Education and Scientific Research (MESRS) are greatly thanked for their financial support, even for making it possible to join the Algerian-French doctoral scholarships program: PROFAS B $^+$ 2019–2020, in order to accomplish and innovate this research work. The authors would like to thank the collaboration of the Institute of Chemistry of Poitiers (IC2MP) for having facilitated the analysis and characterization techniques.

References

[1] M. O. Miranda, B. C. Viana, L. M. Honório, P. Trigueiro, M. G. Fonseca, F. Franco, J. A. Osajima, E. C. Silva-Filho, *Minerals* **2020**, *10*, 132.

[2] L. Qiu, Z. Dong, H. Sun, H. Li, C. C. Chang, *Water Environ. Res.* **2016**, *88*, 1855.

[3] S. Kurwadkar, *Water Environ. Res.* **2019**, *91*, 1001.

[4] D. Kučić Grgić, V. Ocelić Bulatović, M. Cvetnić, Z. Dujmić Vučinić, M. Vuković Domanovac, M. Markić, T. Bolanča, *Water Environ. Res.* **2020**, *34*, 61.

[5] B. S. Choudri, Y. Charabi, *Water Environ. Res.* **2019**, *91*, 1342.

[6] D. Eletto, F. Reppucci, A. Ronga, V. Altieri, S. Brongo, R. Martinelli, M. De Marco, L. Marzullo, *J. Cell Physiol.* **2021**, *236*, 2616.

[7] S. Salvestrini, J. Jovanović, B. Adnadjević, *Desalin. Water Treat.* **2016**, *57*, 22868.

[8] B. Chen, X. Wang, *J. Food Sci.* **2019**, *84*, 2402.

[9] S. Meephon, T. Rungrotmongkol, S. Puttamat, S. Praserthdam, V. Pavarajarn, *J. Environ. Sci.* **2019**, *84*, 97.

[10] European Food Safety Authority, Review of the existing maximumresidue levels (MRLs) for diuron

according to Article 12 of Regulation (EC) No 396/2005, *EFSA J.* **2011**, *9*, 2324.
[11] J. Neury-Ormanni, C. Doose, N. Majdi, J. Vedrenne, S. Morin, S. Höss, W. Traunspurger, *Invertebr. Biol.* **2019**, *138*, e12272.
[12] S. K. Deokar, G. S. Bajad, P. Bhonde, R. P. Vijayakumar, S. A. Mandavgane, *Waste J. Polym. Environ.* **2017**, *25*, 165.
[13] S. R. Sørensen, R. K. Juhler, J. Aamand, *Pest Manage. Sci.* **2013**, *69*,1239.
[14] T. C. Egea, R. da Silva, M. Boscolo, J. Rigonato, D. A. Monteiro, D. Grünig, H. da Silva, F. van der Wielen, R. Helmus, J. R. Parsons, E. Gomes, *Heliyon* **2017**, *3*, e00471.
[15] M. Khosravi, N. Mehrdadi, G. Nabi Bidhendi, M. Baghdad, *Water Environ. Res.* **2020**, *92*, 588.
[16] P. Bhat, P. R. Gogate, *J. Hazard. Mater.* **2021**, *403*, 123657.
[17] R. M. Ramirez Zamora, R. Seux, *J. Water Sci.* **1999**, *12*, 545.
[18] H. Bel Hadjltaief, M. E. Galvez, M. Ben Zina, P. Da Costa, *Arabian J.Chem.* **2019**, *12*, 1454.
[19] S. Salvestrini, P. Di Cerbo, S. Capasso, *Chemosphere* **2002**, *48*, 69.
[20] M. Atarod, J. Safari, *ChemistrySelect* **2020**, *5*, 8394.
[21] S. E. Hearon, M. Wang, T. D. Phillips, *Environ. Toxicol. Chem.* **2020**, *39*, 517.
[22] I. Feddal, A. Ramdani, S. Taleb, E. M. Gaigneaux, N. Batis, N. Ghaffour, *Desalin. Water Treat.* **2014**, *52*, 2654.
[23] A. Ramdani, S. Taleb, A. Benghalem, A. Deratani, N. Ghaffour, *Desalin. Water Treat.* **2015**, *54*, 3444.
[24] R. Sennour, G. Mimane, A. Benghalem, S. Taleb, *Appl. Clay Sci.* **2009**, *43*, 503.
[25] H. Herbache, A. Ramdani, Z. Taleb, R. Ruiz-Rosas, S. Taleb, E. Morallon, L. Pirault-Roy, N. Ghaffour, *Water Environ. Res.* **2019**, *91*,165.
[26] H. Herbache, A. Ramdani, A. Maghni, Z. Taleb, S. Taleb, E. Morallon, R. Brahmi, *Desalin. Water Treat.* **2016**, *57*, 20511.
[27] J. Madejova, *Vib. Spectrosc.* **2003**, https://doi.org/10.1016/S0924-2031(02)00065-6.
[28] A. Toumi, A. Benyocef, A. Yahyaoui, C. Quijada, E. Morallon, *J. Alloys Compd.* **2013**, *551*, 212.
[29] M. Chauhan, V. K. Saini, S. Suthar, *J. Porous Mater.* **2020**, *27*, 383.
[30] M. Quirantes, R. Nogales, E. Romero, *J. Hazard. Mater.* **2017**, *331*,300.
[31] H. Gallard, J. de Laat, B. Legube, *New J. Chem.* **1998**, *22*, 263.
[32] J. Lapworth, D. C. Gooddy, I. Harrison, J. Hookey, Nottingham,UK, British Geological Survey, 26 pp. (IR/05/049)